AIP Journal of Applied Physics

Joule heating as a technique for obtaining uncoupled soft and hard magnetic phases in a Finemet alloy

P. Gupta, A. Gupta, V. Franco, and A. Conde

Citation: Journal of Applied Physics **101**, 033909 (2007); doi: 10.1063/1.2432480
View online: http://dx.doi.org/10.1063/1.2432480
View Table of Contents: http://scitation.aip.org/content/aip/journal/jap/101/3?ver=pdfcov
Published by the AIP Publishing

Joule heating as a technique for obtaining uncoupled soft and hard magnetic phases in a Finemet alloy

P. Gupta and A. Gupta[a)]
UGC DAE Consortium for Scientific Research, Indore, MP 452017, India

V. Franco and A. Conde
Departamento Física de la Materia Condensada, ICMSE-CSIC, Universidad de Sevilla, P.O. Box 1065, 41080 Sevilla, Spain

(Received 1 March 2006; accepted 23 November 2006; published online 6 February 2007)

A detailed study on the microstructural evolution of the $Fe_{73.9}Cu_{0.9}Nb_{3.1}Si_{13.2}B_{8.9}$ (Finemet) alloy upon Joule heating and its correlation with the magnetic properties is reported. Mössbauer spectroscopy suggests the coexistence of soft nonstoichiometric Fe_3Si and hard iron boride magnetic phases. The uncoupled magnetic character of these phases is evidenced by dc-hysteresis loop measurements. X-ray diffraction results display an excellent agreement with the magnetic characterization. The magnetic contribution of the soft phase has been decreased from 70% to 10% with increasing annealing current and time. The switching field value for the soft magnetic phase is 50 A/m, which is very less as compared to 2000 A/m, for the hard magnetic phase. Existence of uncoupled soft and hard magnetic phases makes these systems suitable for use as magnetic labels.
 [DOI: 10.1063/1.2432480]

I. INTRODUCTION

Amorphous materials are widely used in sensors and security systems. Magnetic labels making use of amorphous ribbons are common in the market and they are used as a merchandise protection. The melt-spun FeSiB amorphous alloy ribbon with small amount of Cu and Nb, commercially known as Finemet alloy, also exhibits giant magnetoimpedance (GMI) effect, and thus have potential applications as miniature magnetic field sensors.[1]

There are numerous results in the literature regarding the crystallization behavior of Finemet-type alloys, either produced by conventional furnace annealing or by Joule heating, and its correlation to magnetic properties.[2,3] The devitrification process in these alloys takes place in two main stages. The first one is associated with the appearance of the nanocrystalline Fe (Si) phase embedded in the remaining ferromagnetic amorphous matrix, while the second stage corresponds to the appearance of boride-type phases with recrystallization phenomena. Nanocrystalline samples with an optimal crystalline fraction are even softer than their amorphous precursors due to the exchange coupling between the nanocrystals, transmitted by the ferromagnetic matrix.[4,5] The beginning of the second crystallization stage causes an abrupt magnetic hardening of the material due to the high magnetocrystalline anisotropy of the boride-type phases.[2,6–8]

The amorphous-to-nanocrystalline transformation is strictly related to the heating rate at which the transformation is induced.[9] Nanocrystallization renders these alloys extremely brittle. This limits their practical application in transformer cores, etc. Recently, it has been shown that the so-called dc Joule heating technique produces the amorphous to nanocrystalline transformation to occur without significant embrittlement of the specimen.[10] This technique consists of applying an electrical current to the specimen for a few seconds (heating rate ~100 K/s) and exploits the Joule heat released to the sample to induce the crystallization process. This technique can be performed in air without a strong oxidation of the specimens and has been reported to be used as an excellent procedure to achieve optimum magnetic properties in metallic glasses.[11,12]

One of the peculiarities of Joule heated samples is that they present a finer microstructure than conventionally annealed ones, causing the moderate magnetic hardening related to the onset of nanocrystallization to be less detectable and the hardening associated with the second stage less abrupt.[13]

Multiphase materials exhibiting soft and hard zones, that is, with a hysteresis loop whose field derivative shows various peaks (commonly referred in the literature as materials showing various coercivities) were pointed out to be strong candidates to be used as a magnetic label with the big advantage of being a single material.[14–16] The aim of this work is to study the possibility of obtaining a soft+hard magnetic composite in a Finemet alloy by properly selecting the Joule-heating parameters (current and time). For that purpose, the nanocrystallization of amorphous $Fe_{73.9}Nb_{3.1}Cu_{0.9}Si_{13.2}B_{8.9}$ ribbons induced in a controlled way by Joule heating in air is analyzed in detail using the x-ray diffraction (XRD) and Mössbauer spectroscopy techniques. The magnetic properties are determined from dc hysteresis loops and correlated with the microstructural characteristics of the material.

II. EXPERIMENT

The present study was performed on amorphous ribbons of composition $Fe_{73.9}Nb_{3.1}Cu_{0.9}Si_{13.2}B_{8.9}$, which were produced by rapid quenching and kindly supplied by Dr. P. Duhaj, Solvak republic. Joule heating was made by passing a

[a)]Electronic mail: agupta@csr.ernet.in

constant dc through the sample. The samples were fixed at sample holder by its extremities using brass clamps (heat sinks) at which the current source is connected through a timer. The setup allows to use specimens of different lengths by adjusting the brass clamps. In the present study Joule heating was made on the specimens having identical size ($7\ \text{cm} \times 1\ \text{cm} \times 18\ \mu\text{m}$). The cross section is a fundamental parameter in the Joule heating procedure, since it determines the total dissipated power during the annealing. Annealings were done at constant currents of 6.2, 7.0, and 7.8 A for different times to obtain series of samples at different stages of crystallization. The estimate of the real temperature of the sample during Joule heating is a complex problem[17] as it is a nonisothermal treatment and the short effective time necessary to cause the main structural transformations (generally a few seconds) brings restrictions on direct methods of temperature measurement. Thus in the present work the different crystallization stages are treated as dependent on the annealing parameters (current and time), instead of the temperature of the sample.

X-ray diffraction measurements were performed using Cu $K\alpha$ characteristic radiation from a Rigaku rotating anode generator. A curved crystal diffracted beam monochromator was used to eliminate the iron fluorescence radiation.

In order to get information about the magnetic properties of the specimens room-temperature Mössbauer measurements were made using a ^{57}Co:Rh source in transmission geometry. The obtained spectral profiles were analyzed by means of a current minimization routine, referring the velocity scale and the isomer shifts to metallic iron.

Quasistatic *M-H* hysteresis loops were measured at room temperature for all the as-quenched and Joule heated samples using a quasistatic loop tracer described elsewhere,[18] applying a maximum field of 7 kA/m. Due to the specific design of this equipment, the first derivative of the magnetization curve is directly measured.

III. RESULTS AND DISCUSSION

A. XRD measurements

Figure 1 shows selected XRD spectra, illustrating the microstructural evolution of the samples as a function of annealing current and time. The as-quenched specimen presented a broad hump, which is characteristic of the typical amorphous phase that can be fitted by a Lorentzian function with full width at half maximum of $5.44° \pm 0.04°$. XRD patterns of the annealed specimens show that after treatment with current of 6.2 A (which is the lowest current used for the present studies) for 180 s the specimen becomes crystalline and comprises of nonstoichiometric DO_3 Fe_3Si phase as indicated by sharp peaks at 2θ values of 27.3°, 45.1°, 65.6°, and 83.3° with some small indication of amorphous phase.[19] The line broadening of the crystalline component was then used to determine the average grain size of the nonstoichiometric Fe_3Si phase. The position of the crystalline peaks corresponding to nonstoichiometric Fe_3Si phase remains nearly unchanged for the whole range of annealing current ($6.2\ \text{A} < I < 7.8\ \text{A}$).

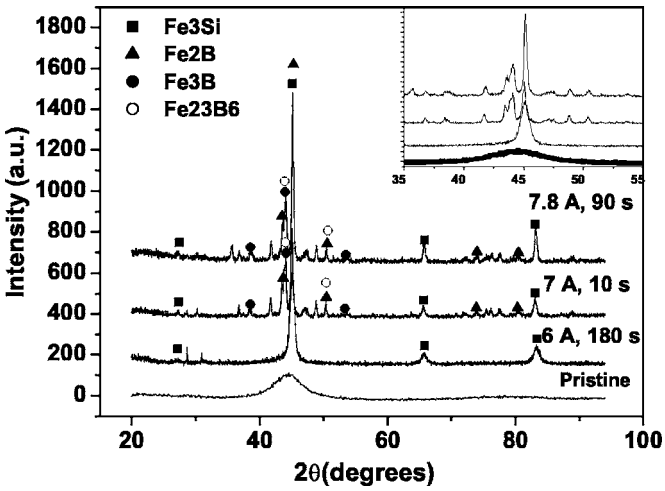

FIG. 1. Some representative XRD patterns of the specimen $Fe_{73.9}Cu_{0.9}Nb_{3.1}Si_{13.2}B_{8.9}$ after annealing at 6, 7, and 7.8 A for different times; unidentified peaks correspond to oxide phases as the ribbons were annealed in air only. For comparison XRD pattern of the as prepared spectra is also shown.

After annealing at 7 A for 10 s, the peak corresponding to (220) reflection of nonstoichiometric Fe_3Si phase becomes sharper, showing no evidence of the remaining amorphous phase. The additional peaks at 43.4°, 50.4°, 73.7°, and 80.2° start appearing which correspond to Fe_2B phase[20] whereas peaks at 38.4°, 44.1°, and 53.7° correspond to Fe_3B phase and peaks at 44.1° and 50.3° are instructive of $Fe_{23}B_6$ phase.[21] XRD pattern of specimen after annealing at highest current of 7.8 A for 90 s also shows signature of coexistence of hard magnetic iron boride phases (Fe_2B, Fe_3B, and $Fe_{23}B_6$) along with soft magnetic nonstoichiometric Fe_3Si phase.

Some of the unidentified XRD lines could correspond to oxide phases, as the ribbons were annealed in air. Since XRD measurements were done in reflection geometry the contribution of surface oxides is expected to be enhanced.

In order to obtain the lattice parameter and particle size of the nonstoichiometric Fe_3Si phase, Rietveld analysis of the annealed samples assuming only nonstoichiometric Fe_3Si phase (i.e., peaks at 27.3°, 45.1°, 65.6°, and 83.3° only were fitted) have been done. The lattice parameter is indeed changing from 5.67 to 5.69 Å as we go on increasing the annealing current; it may be due to some compositional changes in the nonstoichiometric Fe_3Si phase. In fact, a decrease in Si content could be associated with an increase in lattice parameter.[22]

Assuming pseudo-Voigt line profiles full width at half maximum (FWHM) of the maximum intensity peak (nonstoichiometric Fe_3Si phase) in all the samples has been calculated using the formula of Caglioti *et al.*[23] The crystallite size of this phase has been calculated by means of Scherrer formula[24] using peak position and FWHM of the sharpest peak. The crystallite size after annealing at 6.2 A for 180 s is 10.4 ± 0.2 nm which goes on increasing with annealing current and reaches to 27.4 ± 0.1 nm after annealing at 7.8 A for 90 s.

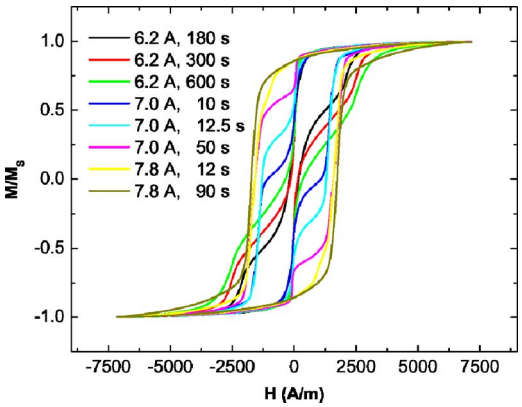

FIG. 2. (Color online) The evolution of hysteresis loops with increasing annealing current.

B. Hysteresis loop measurements

The coercivity of the as-cast specimen is ~18 A/m, a typical value for this kind of alloys before stress relaxation. Upon Joule heating for the selected currents and times, hysteresis loops present evidences of the coexistence of different uncoupled magnetic phases (Fig. 2), as indicated by the fact that the loops could be decomposed in two additive loops with different coercivities. Taking into account the previously described microstructure, the soft magnetic phase should be ascribed to the nonstoichiometric Fe_3Si nanocrystals, while the hard phase should be associated with the boride-type phases. In order to discard the influence of the clamps at both ends of the sample on the existence of the soft magnetic phase, measurements were repeated after removing 1 cm of the samples at both ends, obtaining the same results. Figure 3 presents the evolution of the coercivity of the major loops, H_c, reduced remanence, M_r/M_s, and mean grain size of the nonstoichiometric Fe_3Si phase, $\langle D \rangle$, as a function of annealing conditions. The progressive increase in coercivity upon annealing is not correlated to the mean grain size of the Fe–Si nanoparticles, but to the increasing fraction of boride-type phases, which in the magnetic measurements can be estimated from the relative importance of the different peaks in the derivative of the magnetization curve (Fig. 4). In particular, the sample heated at 7.8 A for 12 s presents a smaller crystallite size than the sample annealed at 7 A for 50 s, although coercivity behavior is the opposite, in agreement

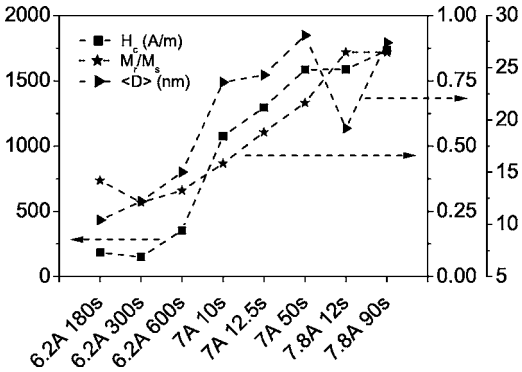

FIG. 3. Dependence on the annealing conditions of the coercivity, reduced remanence, and Fe,Si phase mean grain size of the studied samples.

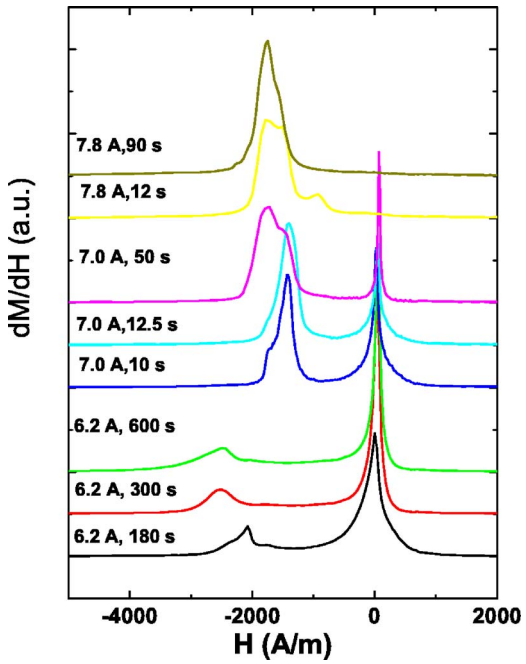

FIG. 4. (Color online) Field derivative of the magnetization curve (second quadrant) of all samples. Vertical displacement is included to avoid the overlapping of the curves.

with the increasing fraction of boride phases evidenced by microstructural and magnetic results. For the annealing at higher currents and times, the hysteresis loops evidence the magnetic coupling between the different phases, with the disappearance of the low-field peak in the field derivative of the magnetization curve.

In order to make an estimation of the relative contributions to magnetization arising from the soft and hard phases, a phenomenological approach can be used. If the loops presented plateaus of magnetization for field values close to the coercivity of the soft phase, the M_r/M_S could have been used for this estimation. However, although there is a notable change in slope close to the coercivity of the soft phase, a horizontal plateau is not found. Consequently, an alternative method, based on a phenomenological fitting of the magnetization curves, has been used. Figure 5 represents a fit of the

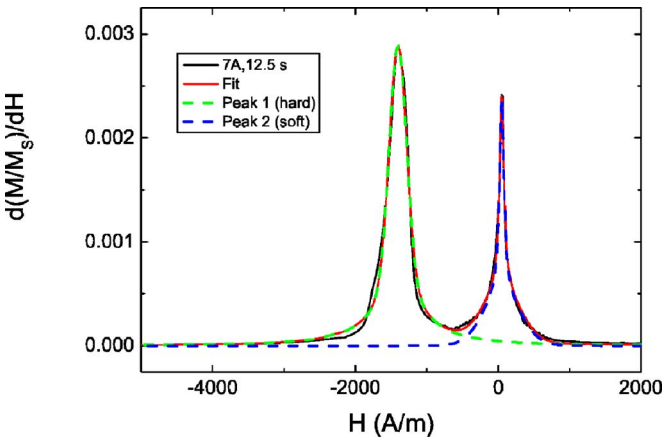

FIG. 5. (Color online) Fit of the normalized magnetization curve corresponding to sample annealed at 7 A for 12.5 s with two pseudo-Voigt functions.

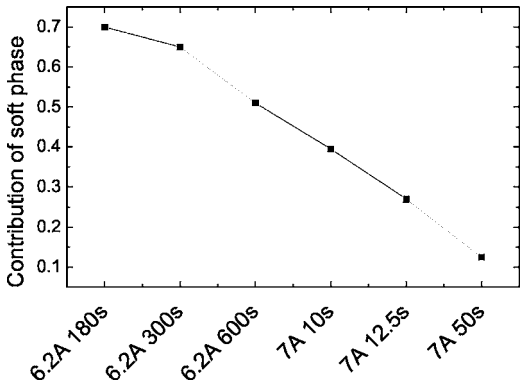

FIG. 6. Contribution of the soft magnetic phase with increasing annealing current and time.

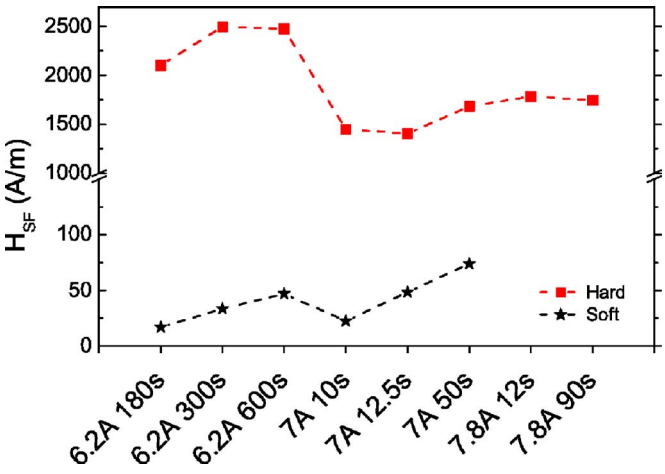

FIG. 7. (Color online) Plot of switching fields corresponding to each phase for all the samples.

normalized magnetization curve with two pseudo-Voigt functions. One represents the uncoupled soft magnetic phase; the other, the hard contributions (only one fitting has been presented as an example). As the loops were previously normalized, the total area under the curve should be 2. Therefore, the area of the soft peak divided by 2 corresponds to the fraction of magnetization emerging from the uncoupled soft phase. If the saturation magnetization of all phases were the same, this would correspond to the volume fraction of the soft phase. The soft phase is fitted more accurately than the hard contribution. This can be due to the diversity of boride phases present in the sample and to the more than probable differences in their coupling. However, as the relevant parameter is the fraction of soft phase and the total curve area is normalized, the nonperfect fitting of the hard contribution is not a real difficulty for the estimation.

From the relative area of the "soft peak," its contribution to the total magnetization can be estimated (Fig. 6). It should be noted that we refer to an uncoupled soft phase, but not to the nonstoichiometric Fe_3Si nanocrystals. For sure there are nonstoichiometric Fe_3Si nanocrystals in the samples above 7 A 50 s, but they cannot be deconvoluted from the magnetization curves, indicating that the phase is coupled to the hard magnetic phase.

Regarding the switching fields of the phases, they can be estimated from the peaks in the field derivatives of magnetization. For the soft phase, its value remains fairly constant with current annealing (Fig. 7). However, the position of the peak for the hard phases does not follow a clear trend. This can be due to the different boride-type phases present in the samples and to their different coupling among them.

With respect to the evolution of the reduced remanence, it is in agreement with that found for conventionally annealed Finemet-type alloys.[25] For the annealing at the highest currents, it tends to 0.85, which is characteristic of randomly oriented cubic particles.[26] Taking into account that the only cubic phases identified in the microstructural analysis are nonstoichiometric Fe_3Si and $Fe_{23}B_6$, they should be responsible for the magnetic behavior of the more crystallized samples, although other boride phases with uniaxial anisotropy are also present.

Finemet alloy, furnace annealed at different temperatures, did not exhibit uncoupled magnetic phases, the reason being as follows: The soft/hard uncoupled behavior is expected to be observed when the volume fraction of both soft (Fe–Si) and hard (Fe–B) magnetic phases is small, so that the coupling among them is weak. In current annealed samples the sample temperature rises to such a high value that both nonstoichiometric Fe_3Si and Fe–B phases (i.e., first and second stages of crystallization) start forming almost simultaneously, and by controlling the annealing time their volume fractions can be controlled. On the other hand in the furnace annealed samples, where annealing times are generally large and annealing temperatures are not very high, initially the first stage of crystallization only is completed and then only the second stage starts. Therefore, it is difficult to realize a situation where both the phases are present in small quantities.

C. Mössbauer measurements

The Mössbauer spectroscopy, a technique based on hyperfine interactions, provides information about local neighborhood of certain probe sites and can distinguish lattice sites, which are atomically, electronically, or magnetically inequivalent. The width of hyperfine field distribution of Mössbauer spectrum depends mainly on the chemical short-range order, thus it can be utilized to identify phases whose dimensions are too small for XRD measurements.

In the present study, the fitting of the Mössbauer spectra has been performed using the NORMOS program, which allows a simultaneous fit of several crystalline spectra with possible addition of an amorphous phase. The specimen is characterized by a distribution of hyperfine fields.[27]

Figures 8 and 9 show respectively, Mössbauer spectrum of as-quenched specimen and some representative Mössbauer spectra of the specimen annealed for 6.2, 7, and 7.8 A for different times. The as-quenched specimen consists of a broad sextet typical of amorphous phase (Fig. 8); the spectrum has been analyzed in terms of a distribution of hyperfine fields representing the distribution of local environment around the Fe atoms. As indicated from the inset of the Fig. 8, the hyperfine field distribution consists of two broad humps. The smaller hump around BHF (magnetic hyperfine

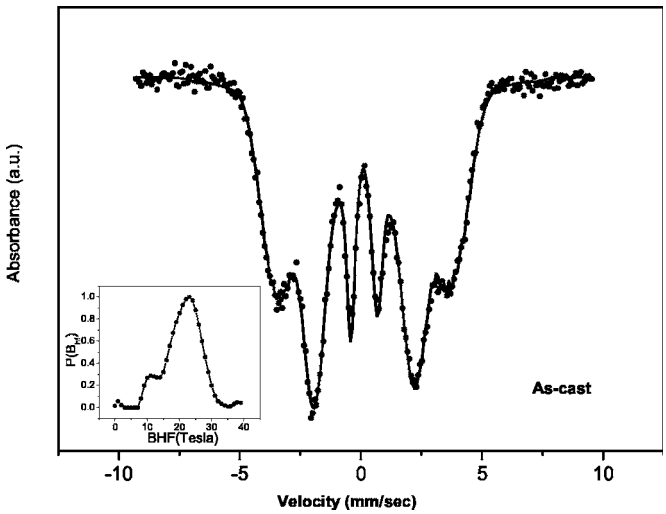

FIG. 8. Room temperature Mössbauer spectrum of the as-quenched $Fe_{73.9}Cu_{0.9}Nb_{3.1}Si_{13.2}B_{8.9}$ alloy; inset shows corresponding hyperfine field distribution.

field)=10 T represents the Fe atoms having Nb near neighbors. It is known that the presence of Nb in the first coordination shell of Fe significantly reduces the hyperfine field of Fe atoms.

The Mössbauer spectra of the annealed specimens show clear evidence about the crystallization (Fig. 9). Thus the spectra after crystallization were best fitted by five overlapping sextets: a broad sextet corresponding to the remaining amorphous phase and four relatively sharp sextets indicating the existence of five distinct Fe sites.

The fitting of the Mössbauer spectra for the sample annealed at 6.2 A for 180 s yields following information:

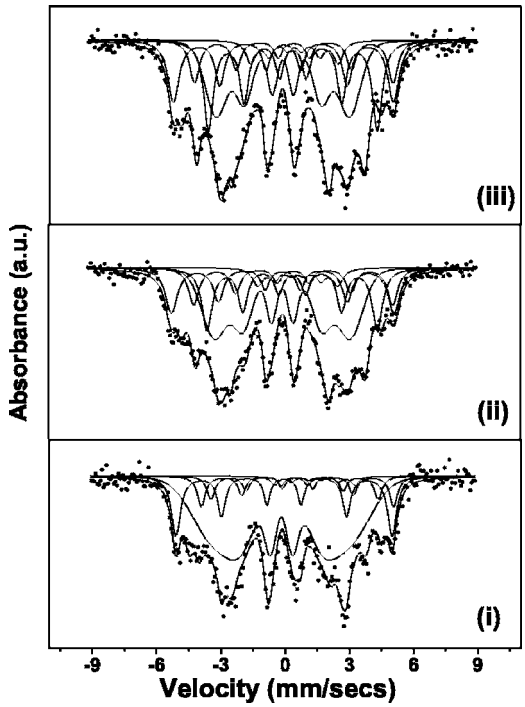

FIG. 9. Some representative room temperature Mössbauer spectra of $Fe_{73.9}Cu_{0.9}Nb_{3.1}Si_{13.2}B_{8.9}$ alloy joule heated at (i) 6.2 A for 180 s, (ii) 7 A for 10 s, and (iii) 7.8 A for 90 s.

(i) About 35% of the Fe is in the amorphous phase.
(ii) Simultaneous presence of the hyperfine field components of 31.3±0.1, 24.2±0.2, and 27.8±0.2 T suggests that the nonstoichiometric Fe_3Si phase is a partially ordered DO_3 structure.[28]

The spectrum has been fitted closely by the internal magnetic field, BHF value of 11.7 T for the one crystalline sextet, which corresponds to β-FeB phase.[29] Other crystalline sextets fitted well with the BHF value of 31.3±0.1, 24.2±0.2, and 27.8±0.2 T correspond to partially ordered nonstoichiometric Fe_3Si DO_3 phase. It is important to note that partially ordered and nonstoichiometric phase is associated with the field values of 20.1, 31.0, 24.3, and 28.5 T.[28]

After annealing for a higher current of 7 A for 10 s the specimen consists of Fe_3Si and Fe–B phases with a crystalline fraction of ~61.9%. However, the spectrum has been best fitted with crystalline sextets having internal magnetic field BHF of 32.1±0.1, 28.8±0.1, 24.6±0.1, and 11.6±0.1 T corresponding to Fe_3Si, Fe_3B, $Fe_2B/Fe_{23}B_6$, and FeB phases, respectively.[30–32]

It is important to note that field values 28.8 and 24.6 T which corresponds to Fe_3B and $Fe_2B/Fe_{23}B_6$ hard magnetic phases, are close to that of Fe_3Si phase. These overlapping field values suggest that the phase may be either Fe_3Si phase or $Fe_2B/Fe_{23}B_6$ phase. But the additional field contribution of 11.6 T gives clear indication of the presence of Fe–B phase.

The presence of all the mentioned phases is still observed after annealing at 7.8 A for 90 s (highest current used in the present study), with a crystalline fraction ~64.4%, thus the specimen is still having different magnetic phases. However, the dc hysteresis measurements show that after annealing at 7.8 A the loops are having single coercivity, although the sample still has both the silicide as well as boride phases. These results can be understood by considering that the single high coercive loop after annealing at 7.8 A is a result of exchange coupling between the phases.

As depicted by Mössbauer measurements, the coexistence of boride phases (Fe_2B, Fe_3B, and $Fe_{23}B_6$) and Fe_3Si phase has also been confirmed with XRD measurements. However, the presence of Fe–B hard magnetic phase has not been detected through XRD measurement while Mössbauer measurements also supports the presence of the same in all the annealed specimens. It may be due to smaller dimension of Fe–B hard magnetic phase for XRD measurements.[33]

IV. CONCLUSIONS

The crystallization process of the $Fe_{73.9}Cu_{0.9}Nb_{3.1}Si_{13.2}B_{8.9}$ specimen produced by Joule heating has been studied by means of x-ray diffraction, Mössbauer spectroscopy, and dc-hysteresis loop measurements. Correlation between structural and magnetic measurements has been found. For the selected annealing currents and times, the samples are comprised of nonstoichiometric Fe_3Si nanocrystals and boride-type phases (FeB, Fe_2B, Fe_3B, and $Fe_{23}B_6$), as identified by XRD and Mössbauer spectroscopy. Their magnetic behavior is characteristic of a composition of uncoupled soft and hard magnetic phases. This feature can be

applied for the production of magnetic labels. In the case of conventional furnace annealing, initially the first stage of crystallization is completed and then only the second stage starts, therefore it is difficult to realize the situation where both the phases are present in comparable quantities.

ACKNOWLEDGMENT

One of the authors (P. Gupta) would like to thank CSIR, New Delhi, for financial support in the form of senior research fellowship.

[1]Z. C. Wang, F. F. Gong, X. L. Yang, L. Zeng, G. Chen, J. X. Yang, S. M. Qian, and D. P. Yang, J. Appl. Phys. **87**, 4819 (2000).
[2]Y. Yoshizawa, S. Oguma, and K. Yamauchi, J. Appl. Phys. **64**, 6044 (1988).
[3]M. E. McHenry, M. A. Willard, and D. E. Laughlin, Prog. Mater. Sci. **44**, 291 (1999).
[4]G. Herzer, IEEE Trans. Magn. **25**, 3327 (1989).
[5]A. Hernando, M. Vázquez, T. Kulik, and C. Prados, Phys. Rev. B **51**, 3581 (1995).
[6]P. Gorria, J. S. Garitaonandia, and J. M. Barandiaran, J. Phys.: Condens. Matter **8**, 5925 (1996).
[7]N. Kataoka, A. Inoue, T. Masumoto, Y. Yoshizawa, and K. Yamauchi, Jpn. J. Appl. Phys., Part 1 **28**, 1820 (1989).
[8]T. Kulik and A. Hernando, Mater. Sci. Forum **179**, 587 (1995).
[9]P. Allia, M. Knobel, M. Baricco, P. Tiberto, and F. Vinai, J. Magn. Magn. Mater. **133**, 243 (1994).
[10]S. S. Yoon, S. C. Yu, G. H. Ryu, and C. G. Kim, J. Appl. Phys. **85**, 5432 (1999).
[11]T. Jagielinski, IEEE Trans. Magn. **19**, 1925 (1983).
[12]J. M. Barandiaraán, A. Hernando, and O. V. Nielsen, IEEE Trans. Magn. **62**, 1964 (1986).
[13]R. Houssa, V. Franco, and A. Conde, J. Magn. Magn. Mater. **203**, 199 (1999).
[14]C. Radeloff, G. Rauscher, and H. Warlimont, U.S. Patent No. 4,950,550 (21 August 1990).
[15]C. Moron, C. Aroca, M. C. Sanchez, A. Garcia, and E. Lopez, IEEE Trans. Magn. **31**, 906 (1995).
[16]J. P. Sinnecker, P. Tiberto, M. Vázquez, and A. Hernando, J. Appl. Phys. **82**, 5871 (1997).
[17]P. Allia, M. Baricco, M. Knobel, P. Tiberto, and F. Vinai, Mater. Sci. Eng., A **179**, 361 (1994).
[18]V. Franco, J. Ramos-Martos, and A. Conde, Rev. Sci. Instrum. **67**, 4167 (1996).
[19]K. Keil, J. L. Berkly, and L. H. Fuchs, Am. Mineral. **67**, 126 (1982).
[20]International centre of diffraction data PDF-2 Database, 2002.
[21]U. Herold and U. Koster, Z. Metallkd. **69**, 326 (1978).
[22]W. P. Pearson, *Handbook of Lattice Spacings and Structures of Metals* (Pergamon, Oxford, 1967).
[23]G. Caglioti, A. Paoletti, and F. P. Ricci, Nucl. Instrum. **3**, 223 (1958).
[24]B. D. Cullity, *Elements of X-ray Diffraction* (Addison-Wesley, Reading, MA, 1978).
[25]V. Franco, C. F. Conde, and A. Conde, J. Magn. Magn. Mater. **185**, 353 (1998).
[26]S. Chikazumi, *Physics of Magnetism* (Krieger, Malabar, 1978), p. 249.
[27]R. A. Brand, J. Lauer, and D. M. Herlach, J. Phys. F: Met. Phys. **14**, 555 (1984).
[28]A. Gupta *et al.*, Intermetallics **8**, 287 (2000).
[29]T. Shiajo, F. Itak, H. Takaki, Y. Nakamura, and N. Shikagono, J. Phys. Soc. Jpn. **19**, 1252 (1964).
[30]W. K. Choo and R. Kaplow, Metall. Trans. A **8A**, 417 (1977); G. L. Caer and J. M. Dubois, Phys. Status Solidi A **64**, 275 (1981).
[31]L. Takacs, M. C. Cadeville, and I. Vincze, J. Phys. F: Met. Phys. **5**, 800 (1975).
[32]H. Franke, U. Herold, U. Koster, and M. Rosenberg, in *Rapidly Quenched Metals III*, edited by B. Cantor (Chameleon, London, 1978), p. 155.
[33]F. H. Sanchez, J. I. Budnick, Y. D. Zhang, W. A. Hines, and M. Choi, Phys. Rev. B **34**, 4738 (1986).